Noname manuscript No.
(will be inserted by the editor)

Stereo-DIC uncertainty estimation using the epipolar constraint and optimized three camera triangulation

R. Balcaen · P. L. Reu · D. Debruyne

Received: date / Accepted: date

Abstract Even though stereo-DIC is widely used in the field of experimental mechanics, uncertainty quantification techniques lag behind. Camera motion for example is often neglected, even though it is present and it can introduce bias. We propose to estimate the error caused by camera motion, based on the epipolar distance, by using a 3-camera system. This solves the problem of the lack of sensitivity along the epipolar line by placing a 3rd camera perpendicular, providing sensitivity in both directions. The 3rd camera provides modest improvement on the results with an optimized triangulation.

Keywords Digital image correlation · Uncertainty quantification · Error assessment · Optical techniques

1 Introduction

Uncertainty quantification of any measurement technique is a necessity when the technique is used in practical applications. A measurement is only useful if the

R. Balcaen · D.Debruyne
KU Leuven, Department of Materials Technology, Campus Ghent, Gebroeders Desmetstraat 1, 9000 Ghent, Belgium
E-mail: ruben.balcaen@kuleuven.be

P. L Reu
Sandia National Laboratories, Albuquerque, New Mexico, United States

uncertainty of that measurement is known. However, it is not always easy to determine errors bars since not all measurement techniques are straightforward. Digital image correlation (DIC) is a perfect example of this; the complex optical-numerical measurement chain makes it extremely hard to determine error bounds of a measurement. Much work has been done on quantifying the error for 2D DIC ([1],[2],[3]), however less publications on stereo-DIC uncertainty quantification are available ([4],[5]), due to the extra complications introduced by the calibration, cross-correlation and triangulation. We present a novel method for estimating the error bounds of a stereo-DIC measurement with camera motion, based on the epipolar constraint and a three camera optimized triangulation. This technique can be added to the already existing techniques for estimating the errors during the cross-correlation stage, 2D matching and triangulation as a part of a larger error estimation scheme in order to estimate the total error of a measurement. The validity of the proposed technique is checked with simulated images, generated with an FE-based stereo-DIC image simulator, presented in [6] and used for stereo-DIC uncertainty quantification in [7].

2 The epipolar constraint and uncertainty quantification of stereo-DIC

2.1 Epipolar geometry

We present a novel method for determining the uncertainty zone of a stereo-DIC measurement based on the epipolar constraint. This constraint is illustrated in figure 1. A point in the world space, point X, will be projected onto the camera sensor plane by a perspective projection as X_1 for the left camera (with optical centre O_1), X_2 for the right camera (with its optical center O_2) and X_3 for the top camera (with its respective optical center O_3). The projection of camera 1 (indicated as line X-O_1) is seen by camera 2 as the line e_2-X_2. This line is called the epipolar line and is indicated as a green line on figure 1 in camera 2. The epipolar line limits the possible location of a 3D point to a single line in camera

frame 2 if the projection of that point is known in camera 1 and if the relative camera orientation is known. The same applies to camera system 1-3, resulting in the vertical oriented epipolar lines (indicated in blue). The epipolar constraint is already used in computer vision for determining camera orientation based on corresponding points ([8],[9]) or for limiting the search for point correspondance since they must lie on the epipolar line ([10],[11]). That is, only a search along the epipolar line must be performed for finding the corresponding point in camera 2 if the location of X_1 in camera 1 is known.

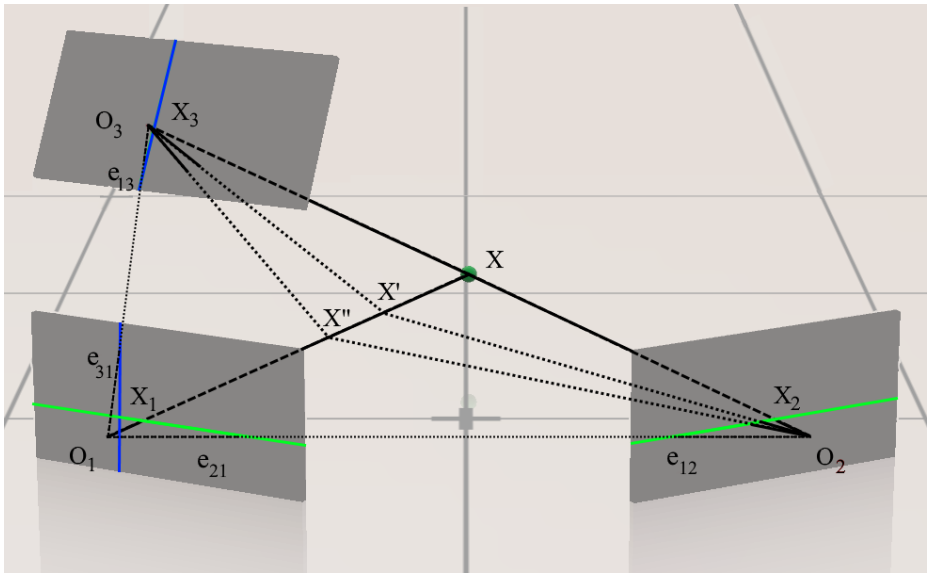

Fig. 1: Epipolar geometry for a 3 camera system.

This constraint can also be used for checking the quality of calibration by reporting the distance of a matched point to the epipolar line, as implemented in the commercial MatchID DIC package [12]. A large epipolar distance indicates a potential error in the camera calibration. However, we can further exploit this constraint since the epipolar distance will change during an experiment due to camera motion. We explore if error bars of a DIC measurement can be determined by eploiting this change in epipolar distance. This approach is particularly useful

when there are no stationary objects in the FOV to measure the camera motion. Other methods of correcting for camera motion may be more appropriate if stationary objects are available [13], however there are many experiments where this is not possible.

2.2 Uncertainty quantification based on the epipolar distance

Let point X_1 in camera 1 have the integer pixel location (x,y) in the reference image. After tracking this point over different frames it will have a displacement of (u,v), placing this point at ($x + u$, $y + v$) in the image of the deformed state in camera 1. Its corresponding point in camera 2 is denoted as ($x + q$, $y + r$) in the reference frame (with q and r being the displacement obtained from a 2D-DIC cross-correlation between cameras) and ($x + u + q$, $y + v + r$) in the image of the deformed state (in which q and r are updated). In a normal stereo-DIC analysis the corresponding points in both camera frames will be combined with the calibration data to perform a triangulation. We now assume that the reported epipolar error (E_e) obtained after triangulation is a measure of the camera motion, and therefore the calibration error, which will result in a bias in the results. We will use the measured maximum epipolar error (E_e) during an experiment as a worst case estimation of the calibration error. Using this error with the assumed perfect cross-correlation, we can estimate the influence of this error on the triangulated point by using equation 1.

$$(x + u + q \pm E_e, y + v + r \pm E_e) \tag{1}$$

An error region can then be determined in which all the data points must lie by using the updated locations and equation 1 for triangulation. Please note that this assumes that images are taken with a stationary setup for determining the error region, which is not the case in a real experiment. Also note that this method will only be valid if there is motion away from the epipolar line; if the corresponding

point in the right camera frame moves along the epipolar line no epipolar error will be indicated. We first illustrate the epipolar problem with only a 2-camera system. Simulated images are created of camera 1 and 2 in the setup depicted in figure 1 that is undergoing camera rotation. Four cases will be discussed; both cameras rotate up with the same angle, only one camera moves up while the other remains static, both cameras rotate with the same angle (however in an opposite direction) and both cameras rotate away from each other along the epipolar line. The imposed angles are values that were obtained experimentally for a previous paper concerning the influence of camera motion on stereo-DIC [14].

1. **Both cameras rotate up with the same angle.** No epipolar error is detected in this case since the stereo-rig undergoes rigid body rotation. The resulting biased displacement field is caused by the rotation of the reference frame, and can be corrected for by removing rigid body motion. Therefore, no bias is predicted (after rigid body motion removal) in table 1, setting the displacement field within its normal bounds that are predicted by a noise evaluation.
2. **Static left camera and the right camera rotates up.** An epipolar distance change is measured between the unmoved reference and the moved system as can be seen in table 1. By applying the proposed method an error bound can be predicted that encompasses this error.
3. **Left camera rotates down and right camera rotates up with the same angle.** In this the cameras rotate the same angle, however in opposite directions. The epipolar distance change and the corresponding estimated error bound will be doubled compared to case 2, as could be expected..item **Cameras rotate away from each other along the epipolar line.** Here we focus on what happens if both cameras rotate along the epipolar line, not generating an epipolar distance change. A bias in U (the in-plane horizontal direction) of 0.037mm (=0.5pixels) was obtained and bias in the out-of-plane direction of 0.207mm was obtained. This while no bias is predicted by the proposed method

since the movement is along the epipolar line, thus not generating an epipolar error and therefore undetectable.

Good correspondence is obtained for test cases 1-3, verifying the validity of the technique for movement away from the epipolar line. Case 4 however does not predict a bias, even though one is present. This is due to the insensitivity of the epipolar distance when moving along the epipolar line. This illustrates that a 3rd camera will be required to correctly estimate E_e in all possible cases. The principle of a 3 camera system and an optimized triangulation routine is introduced in the next section.

Table 1: Example cases and error estimation

case	rotation angle camera 1	rotation angle camera 2	E_e [pixels]	resulting bias [mm]	predicted bias [mm]
1	0.002° up	0.002° up	0.0057	≈ 0	≈ 0
2	0.0°	0.002° up	0.44	0.018 in V (= 0.25 px)	±0.018 in V
3	0.002° down	0.002° up	0.88	0.036 in V (= 0.50 px)	±0.037 in V
4	0.002° left	0.002° right	≈ 0	0.207 in W	≈ 0

3 Three camera optimized stereo-DIC uncertainty quantification

3.1 Optimized three camera triangulation

Case 4 in the previous section indicated a large bias in both U and W, without an indication of a bias by the proposed method. This is due to the lack of an epipolar distance change since the epipolar constraint is insensitive to motion along the epipolar line. In order to solve this problem a third camera is introduced, placed vertically above the first camera (as can be seen in figure 1 and 2). This yields a second, orthogonal epipolar line. This third camera will detect the motion of the horizontal camera pair along their respective epipolar lines. The insensitivity of motion along the epipolar line of the horizontal camera pair is solved by

constructing the vertical uncertainty bar based on the epipolar change from the horizontal camera pair and the vertical camera pair will be used for constructing the horizontal uncertainty bar. A conservative approach is followed for determining the out-of-plane uncertainty by using the largest out-of-plane error bar from both camera systems.

Having a third camera will also introduce the possibility of implementing an optimized triangulation routine by using the data of all cameras simultaneously. Normally only two corresponding points are available for triangulation, however, having a third camera will yield a third corresponding point that can be used for further improving the triangulation. This proposed optimized triangulation minimizes the total back-projection error, defined as the sum of the difference between the projection of the proposed 3D point in space on a image-plane and the corresponding image-plane point as given by the DIC-routine [15].

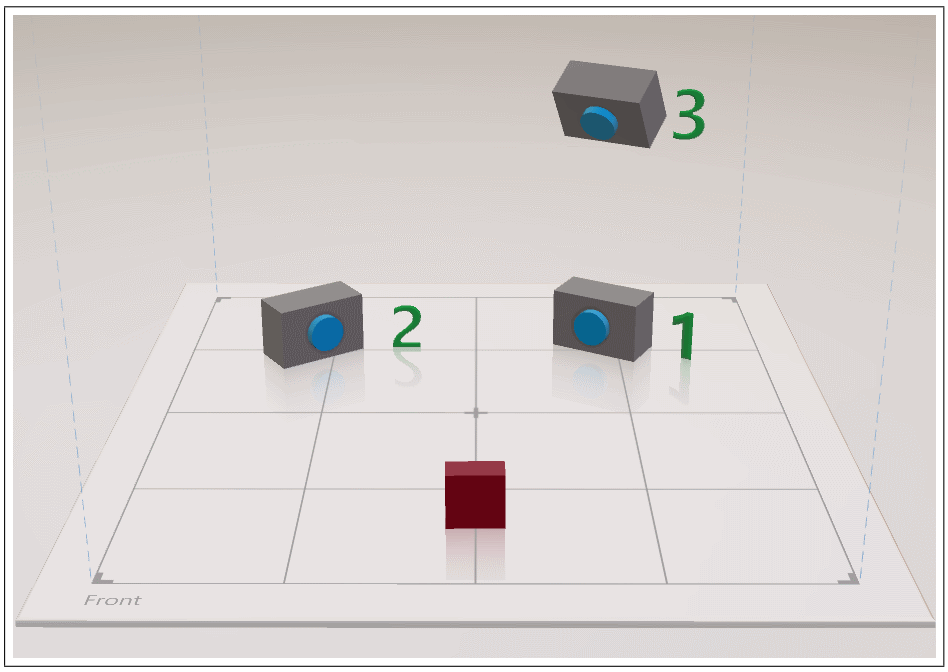

Fig. 2: Camera setup and target in front.

Let X be a 3D point in space, and let $x_1, x_2, \ldots, x_n$ be the projections of point X in the camera frame of camera n by: $x_n = P_n X$. Each projection (defined by projection matrix P_n) yields an x_n, which has the pixel locations of (i_n, j_n), while the true projection of the point (as given by the matched points by using DIC) has a pixel location of $(i_n^{'}, j_n^{'})$. Let us now define the total reprojection error function E_{total} as:

$$E_{total} = \sum_{i}^{n} \left((i_n^{'} - i_n)^2 + (j_n^{'} - j_n)^2 \right) \tag{2}$$

By minimizing equation 2 with $n = 3$ in this case, the optimal 3D point can be identified, given the corresponding points (obtained with DIC). Since a third camera introduces extra restrictions a better overall 3D location is obtained, especially when camera motion is present. The improvement with a third camera for a setup with little camera motion is however modest, making it superfluous to have a third camera when one does not want to determine error bounds and the third camera is only used for increasing the precision and accuracy of the measurements by improving the triangulation stage.

3.2 Results

The three camera optimized triangulation is combined with the earlier presented error estimation theory and verified by simulating an experiment in which there is camera rotation present around all axes. The considered setup can be seen in figure 2 and the details are outlined in table 2. The uncertainty region is first calculated, based on the worst possible rotation combinations and their corresponding epipolar distance changes (E_e). Consider this as the highest epipolar distance change you would measure in a real experiment. This is followed by letting the cameras rotate randomly around all axes simultaneously, within the predefined bounds, which are set in this case at ± 0.0015 (realistic rotation angles as measured by the authors [14]).

Table 2: Three camera optimized triangulation and error estimation validation setup

Parameter	Value
Stereo angle camera 1-2 [°]	20
Stereo angle camera 1-3 [°]	20
Maximum camera rotation [°]	0.0015
Focal length lenses [mm]	16, 50
Field of view [mm]	131.6x100
Camera resolution [pixels]	1624x1234
Pixel to mm conversion [μm/pixel]	80
Camera noise level [%]	0.5

Table 3: DIC settings for identifying corresponding points in all cameras

Parameter	Value
Subset size [pixels]	21
Step size [pixels]	10
Interpolation	B-spline
Shape function	affine

50 Image-triplets are generated and the corresponding points in all cameras are identified by performing a DIC analysis (the DIC settings can be found in table 3) and based on these corresponding points, and the perfect calibration data (as exported by the simulator), the points are triangulated in 3D space with the proposed optimized three camera triangulation. The measured displacements (which should be equal to zero, but are biased due to camera rotation) are averaged over the FOV and these must lie within the earlier defined uncertainty region since all cameras rotate within the predefined bounds and since the worst combination of these bounds was used to calculate the uncertainty region. Figures 3 and 4 project the uncertainty region, as calculated with the proposed method, to the X-Y plane (figure 3) and the Y-Z plane (figure 4), together with the average bias of each of the 50 datasets. The proposed method successfully captures all 50 cases for both the setup with 50mm lenses (indicated in red) and 16mm lenses (indicated in blue) if the true, unbiased position is known (indicated as a black cross). It is clear that the error region will be bigger with higher focal length lenses. This is caused by the higher magnification of the lens; a higher stand-off will represent a

higher motion at the target side with the same camera motion. This was earlier indicated in [14]. The unbiased position however will never be known since camera motion will be present and thus any biased instance, e.g. the data point indicated in green, can have its own uncertainty region (as indicated as the green region) that will encompass the true value. This conservative approach results in accurate uncertainty region determination.

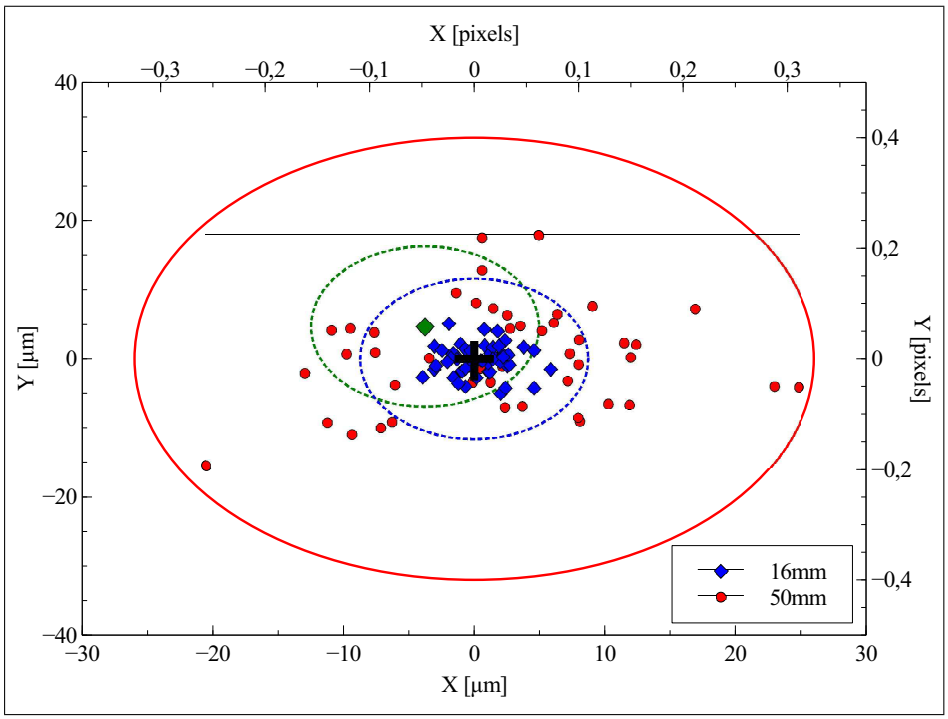

Fig. 3: Projection of the predicted uncertainty region to the X-Y plane.

4 Conclusion

An error region estimation method exploiting the change in epipolar distance is combined with a three camera optimized triangulation for improving DIC measurements. Simple cases in section 2 indicate the working principle and give an indication of the performance in an ideal case. Since the epipolar constraint only

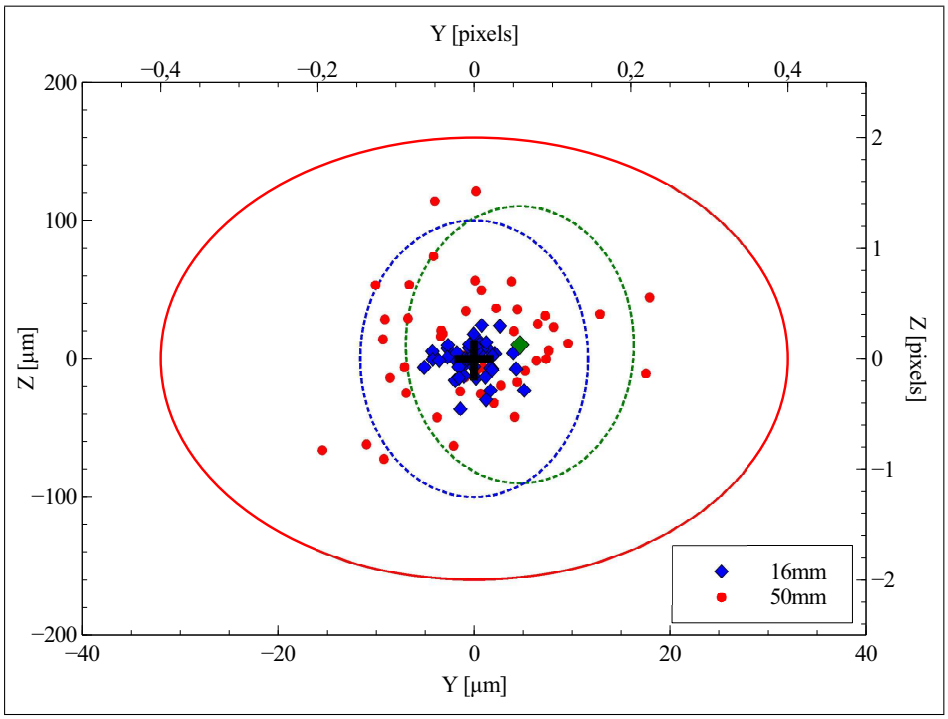

Fig. 4: Projection of the predicted uncertainty region to the Y-Z plane.

gives information regarding changes away from the epipolar line a three camera setup is introduced, yielding extra information due to the orthogonal placement of the epipolar lines. By adding the third camera information on the epipolar distance change in orthogonal directions is available, as well as the possibility to perform an optimized triangulation. Conservative error bounds can be constructed and the validity of the method is proven in section 33.2 with a numerical example. This method therefore provides a technique of estimating bias errors due to camera motion by using the epipolar distance. It also confirms previous statements that the error bounds due to camera rotation increase with higher focal length lenses [14].

References

1. Phillip Reu. A realistic error budget for two dimension digital image correlation. *Advancement of Optical Methods in Experimental Mechanics*, 3:189–193, 2015.
2. Pascal Lava, Steven Cooreman, Sam Coppieters, Maarten De Strycker, and Dimitri Debruyne. Assessment of measuring errors in dic using deformation fields generated by plastic fea. *Optics and Lasers in Engineering*, 47(7-8):747, 753 2009.
3. Pascal Lava, Wim Van Paepegem, Sam Coppieters, l De Baere, Yueqi Wang, and Dimitri Debruyne. Impact of lens distortions on strain measurements obtained with 2d digital image correlation. *Optics and lasers in Engineering, 51(5): 576-584*, 2013.
4. Y.Q. Wang, M.A.Sutton, X. D. Ke, H. W. Schreier, P. L. Reu, and T. J. Miller. On error assessment in stereo-based deformation measurements-part 1. *Experimental mechanics*, 51(4):405–422, April 2011.
5. X. D. Ke, H. W. Schreier, M. A. Sutton, and Y. Q. Wang. On error assessment in stereo-based deformation measurements-part 2. *Experimental mechanics*, 51(4):423–441, April 2011.
6. R. Balcaen, L. Wittevrongel, P.L. Reu, P. Lava, and D. Debruyne. Stereo-dic calibration and speckle image generator based on fe formulations. *Experimental Mechanics doi:10.1007/s11340-017-0259-1*, 2017.
7. R. Balcaen, P.L. Reu, P. Lava, and D. Debruyne. Stereo-dic uncertainty quantification based on simulated images. *Submitted to Experimental Mechanics*, 2016.
8. A. Cefalu, N. Haala, and D. Fritsch. Structureless bundle adjustment with self-calibration using accumulated constraints. *ISPRS Annals of Photogrammetry, Remote Sensing and Spatial Information Sciences*, 3(3):3–9, 2016.
9. T. Dang, C. Hoffman, and C. Stiller. Continuous stereo self-calibration by camera parameter tracking. *IEEE Transactions on Image Processing*, 18(7):1536–1550, July 2009.
10. W. Hoff and N. Ahuja. Surfaces from stereo: integrating feature matching, disparity estimation, and contour detection. *IEEE Transactions on Pattern Analysis and Machine Intelligence*, 11(2):121–136, Februari 1989.
11. M. S. Lew, T. S. Huang, and K. Wong. Learning and feature selection in stereo matching. *IEEE Transactions on Pattern Analysis and Machine Intelligence*, 16(9):869–881, September 1994.
12. http://www.matchidmbc.com/.
13. T. J. Miller, H. W. Schreier, and P. L. Reu. High-speed dic data analysis from a shaking camera system. In *SEM annual conference*, 2007.
14. R. Balcaen, P.L. Reu, P. Lava, and D. Debruyne. Influence of camera rotation on stereo-dic and compensation methods. *Submitted to Experimental Mechanics*, 2017.

15. H Stewenius, F Schaffalitzky, and D Nister. How hard is 3-view triangulation really? *IEEE Computer Vision*, 2005.